




ARTICLE



Probing midbrain dopamine function in pediatric obsessive-compulsive disorder via neuromelanin-sensitive magnetic resonance imaging

David Pagliaccio^{1,2} [✉], Kenneth Wengler^{1,2} , Katherine Durham^{1,2}, Martine Fontaine^{1,2}, Meryl Rueppel^{1,2}, Hannah Becker³, Emily Bilek³, Sarah Pieper^{1,2}, Caroline Risdon^{1,2}, Guillermo Horga^{1,2}, Kate D. Fitzgerald^{1,2} and Rachel Marsh^{1,2} 

© The Author(s), under exclusive licence to Springer Nature Limited 2023

Obsessive-compulsive disorder (OCD) is an impairing psychiatric condition, which often onsets in childhood. Growing research highlights dopaminergic alterations in adult OCD, yet pediatric studies are limited by methodological constraints. This is the first study to utilize neuromelanin-sensitive MRI as a proxy for dopaminergic function among children with OCD. $N = 135$ youth (6–14-year-olds) completed high-resolution neuromelanin-sensitive MRI across two sites; $n = 64$ had an OCD diagnosis. $N = 47$ children with OCD completed a second scan after cognitive-behavioral therapy. Voxel-wise analyses identified that neuromelanin-MRI signal was higher among children with OCD compared to those without (483 voxels, permutation-corrected $p = 0.018$). Effects were significant within both the substantia nigra pars compacta ($p = 0.004$, Cohen's $d = 0.51$) and ventral tegmental area ($p = 0.006$, $d = 0.50$). Follow-up analyses indicated that more severe lifetime symptoms ($t = -2.72$, $p = 0.009$) and longer illness duration ($t = -2.22$, $p = 0.03$) related to lower neuromelanin-MRI signal. Despite significant symptom reduction with therapy ($p < 0.001$, $d = 1.44$), neither baseline nor change in neuromelanin-MRI signal associated with symptom improvement. Current results provide the first demonstration of the utility of neuromelanin-MRI in pediatric psychiatry, specifically highlighting in vivo evidence for midbrain dopamine alterations in treatment-seeking youth with OCD. Neuromelanin-MRI likely indexes accumulating alterations over time, herein, implicating dopamine hyperactivity in OCD. Given evidence of increased neuromelanin signal in pediatric OCD but negative association with symptom severity, additional work is needed to parse potential longitudinal or compensatory mechanisms. Future studies should explore the utility of neuromelanin-MRI biomarkers to identify early risk prior to onset, parse OCD subtypes or symptom heterogeneity, and explore prediction of pharmacotherapy response.

Molecular Psychiatry (2023) 28:3075–3082; <https://doi.org/10.1038/s41380-023-02105-z>

INTRODUCTION

Obsessive-compulsive disorder (OCD) is an impairing psychiatric condition that is characterized by the presence of obsessions (i.e., intrusive thoughts, images, or urges) and compulsions (i.e., repetitive actions aimed at preventing or reducing distress). A significant body of research has focused on the role of serotonin in OCD [1–4], yet there is growing genetic, neuroimaging, and treatment research highlighting alterations in dopaminergic functioning in adults with OCD [5–8]. Such studies often implicate striatal dopamine hyperactivity via imaging of dopamine transporter or dopamine receptor binding [9–14], though findings are at times mixed or rely on small sample sizes. Such dopaminergic alterations likely contribute to fronto-striatal circuit alterations often implicated in OCD pathophysiology [8].

These findings from human clinical work build on a broader body of research, which highlights the role of dopamine in repetitive behaviors. For example, studies find that dopaminergic drugs can induce repetitive behaviors in patients with Parkinson's Disease, e.g., [15, 16]. Animal models also demonstrate that pharmacological disruption of midbrain dopamine signaling

elevates compulsive-like behaviors [17] as well as similar dopaminergic effects on stereotypy in speech [18] or self-grooming behavior [19]. Theories suggest a potential inverted-U-shaped association between dopamine and normative functioning, i.e., both too much and too little dopaminergic activity could lead to detrimental outcomes [20].

Despite increasing evidence supporting dopaminergic hypotheses in OCD, the invasiveness of methodologies typically used to examine dopamine have limited our ability to probe alterations in pediatric OCD—e.g., the use of positron emission tomography (PET) is generally limited in pediatric research given the need for radiotracer injection. Recently, a safe and non-invasive alternative means of characterizing dopamine has been developed using magnetic resonance imaging (MRI) to assess neuromelanin [21, 22], a key product of catecholamine (e.g., dopamine) metabolism.

The lifecycle of dopamine is complex; briefly, this includes: dopamine is largely produced in the substantia nigra pars compacta (SNpc) and ventral tegmental area (VTA), key midbrain nuclei that project to the striatum, prefrontal cortex, and other

¹Department of Psychiatry, Columbia University Irving Medical Center, New York, NY, USA. ²New York State Psychiatric Institute, New York, NY, USA. ³Department of Psychiatry, University of Michigan, Ann Arbor, MI, USA. ✉email: david.pagliaccio@nyspi.columbia.edu

Received: 9 January 2023 Revised: 26 April 2023 Accepted: 3 May 2023
Published online: 17 May 2023

regions [23–25]. Excess dopamine is metabolized via several pathways [26]; the neuromelanin pathway involves non-enzymatic iron-dependent oxidation and results in neuromelanin-iron complexes accumulating in presynaptic midbrain dopamine neurons [22, 27, 28]. Thus, neuromelanin concentration is dependent on a combination of dopamine production [29], reuptake, and metabolism.

Critically, neuromelanin-iron complexes are paramagnetic and thus create signal hyperintensity with MRI [22, 30]. Accordingly, neuromelanin-MRI has been validated to index neuromelanin tissue concentration in post-mortem human data, as well as to correlate with key striatal outcomes of interest, like striatal dopamine release capacity measured via PET in vivo [21] and D₂ receptor density [31]. Neuromelanin-MRI has excellent test-retest reliability (intra-class correlation > 0.80) [32, 33] and reproducibility across multiple MRI sequences [33, 34].

An increasing number of studies are examining neuromelanin-MRI in adult clinical populations. Several studies have shown sizeable decreases in SNpc neuromelanin-MRI signal in Parkinson's disease [35–45], consistent with the underlying degeneration of SNpc dopamine neurons [46]. Additionally, evidence is coalescing around increases in neuromelanin-MRI signal in schizophrenia [21, 47–53], consistent with hyperdopaminergic theories of psychosis [54]. Overall, neuromelanin-MRI shows great promise as a non-invasive proxy measure of midbrain dopamine function. Whereas methods like PET index one's current state, neuromelanin-MRI likely reflects a summed measure of subtle alterations over time as neuromelanin accumulates gradually over the lifetime [55].

Herein, our goal was to probe midbrain dopamine in pediatric OCD via neuromelanin-MRI. To our knowledge, this is the first study to leverage neuromelanin-MRI in early childhood psychopathology, specifically pediatric OCD. Thus, findings could pave the way toward better understanding of dopamine function in childhood psychiatric disorders. Data were acquired from a relatively large sample of children across two sites; children with OCD underwent rigorous clinical assessment and were offered manualized cognitive behavior therapy (CBT) with exposure and response prevention after MRI scanning. Though prior data is limited, we hypothesized that children with OCD would exhibit elevated neuromelanin-MRI signal in the midbrain, as a proxy for increased dopaminergic function. Using high-resolution MRI, we aimed to parse potential spatial specificity of these findings within the SNpc and VTA, both of which contribute to circuits implicated in OCD pathophysiology [8]. Further analyses aimed to probe dimensional associations with symptom severity and explore dopamine signal in relation to CBT response.

METHODS

Participants

Children (6–14 years old) were recruited for the current study between April 2019 and September 2022 across two sites, Columbia University/New York State Psychiatric Institute (CU/NYSPI) and the University of Michigan (UM). This included treatment-seeking children with OCD and children without OCD. All children were invited to complete interview and questionnaire assessments, cognitive testing, and MRI scanning. Children with OCD were offered CBT [56, 57] (see Supplement) and a subset completed post-treatment MRI scans. Participants were recruited from the New York City, NY and Ann Arbor, MI areas using flyers, internet advertisements, clinician referrals, and word-of-mouth. The broader study was registered on ClinicalTrials.gov (NCT03584945). The Institutional Review Boards of each institution approved this study. Children provided assent and parents/guardians provided written informed consent.

In total, $N = 163$ children attempted MRI scans. Of these, $n = 14$ did not complete neuromelanin-MRI scans (due to time constraints, participant terminating the scan, etc.) and neuromelanin-MRI data were excluded from an additional $n = 14$ for poor data quality. This left $N = 135$ participants for the current analyses ($n = 62$ from CU/NYSPI and $n = 73$ from UM),

including $n = 64$ children with OCD ($n = 31$ from CU/NYSPI and $n = 33$ from UM). Of the $n = 64$ children with OCD, $n = 47$ successfully completed neuromelanin-MRI scans post-CBT ($n = 22$ from CU/NYSPI and $n = 25$ from UM).

Children in the OCD group had a primary diagnosis of OCD, confirmed via clinical interviews, and were excluded for current MDD, completing a prior full course of CBT for OCD, or any ongoing psychotherapy. Children without OCD were excluded for any current or lifetime psychiatric diagnosis; these children could have subclinical obsessive-compulsive symptoms (i.e., symptoms that do not consume ≥ 1 h/day or cause distress or interference). Including children with and without subclinical obsessive-compulsive symptoms allowed us to examine neuromelanin-MRI signal across the non-clinical to clinical range of obsessive-compulsive symptom severity.

All children and parents/guardians were English- or Spanish-fluent; children were excluded for pregnancy, major medical or neurological problems, MRI contraindication, Wechsler Abbreviated Scale of Intelligence IQ score < 80, illicit drug use, active suicidal ideation, a lifetime history of psychotic disorder, bipolar disorder, eating disorder, pervasive developmental disorder, or substance/alcohol abuse. Children without OCD were excluded for psychotropic medication use; children with OCD were excluded for current psychotropic medication use (other than ADHD medications). In the current sample, 3 participants had previously taken SSRI medications, 3 had previously and 4 were currently taking ADHD medications.

Clinical assessment

Children's lifetime and current psychiatric diagnoses were assessed using the Kiddie Schedule for Affective Disorders and Schizophrenia (KSADS) [58]. A trained evaluator assessed patients' current (past week) and lifetime (worst ever) OCD symptom severity using the Children's Yale-Brown Obsessive-Compulsive Scale (CY-BOCS) [59]. An adapted version of the Schedule for Obsessive Compulsive and Other Behavioral Syndromes (SOCOBS) [60] was used in conjunction with the CY-BOCS to assess the history of obsessive and compulsive symptoms (e.g., age of onset, age when symptoms became distressing/interfering) as well as the presence of tic and grooming disorders. Participants also completed self-report on the 21-item Obsessive-Compulsive Inventory-Children's Version (OCI-CV) [61] to measure symptom severity across the full sample.

MRI acquisition

Participants completed MRI scanning on a 3T GE scanner, either a SIGNA Premier with 48-channel head coil at NYSPI and one of two Discovery MR750 scanners with 32-channel Nova head coils at UM. This included a T1w BRAVO structural, aligned with the ABCD Study protocols for GE [62]: flip angle = 8°, TI = 1060, 208 slices, FOV = 256 × 256, TE = 2 ms, TR = 2500 ms, 1 × 1 × 1 mm resolution. Five volumes of neuromelanin-sensitive MRI data were acquired for each participant, using a 2D gradient-recalled echo sequences with magnetization transfer contrast (2D GRE-MTC) adapted from prior work [21, 33, 63, 64]: TE = min, TR = 500 ms, flip angle = 40°, number of excitations (NEX) = 1, MT frequency offset = 1200 Hz, 20 slices, FOV = 220 × 165, matrix = 512 × 320, in-plane resolution = 0.43 × 0.43 mm, slice thickness = 1.5 mm. The restricted FOV was placed based on the T1w structural to ensure midbrain coverage based on validated protocols [33, 64]. Data were visually checked at the scanner and re-run if significant head motion was noted.

MRI processing

Neuromelanin-MRI data were visually checked, and individual volumes were excluded for head motion, ringing, or other artifacts. Participants with insufficient data were excluded (< 3 good quality volumes). Neuromelanin-MRI data were processed with a MATLAB-based pipeline leveraging SPM, AFNI, and ANTs functions as previously described [33], summarized in Supplementary Fig. S1. This included (1) realignment and reslicing of the multiple neuromelanin-MRI volumes to the first volume using SPM; (2) averaging of the neuromelanin-MRI volumes; (3) N4 bias field correction of the T1w structural using ANTs; (4) ANTs brain extraction of the T1w image (NKI 10 and under atlas); (5) non-linear ANTs normalization of the brain-extracted T1w image to MNI space; (6) ANTs rigid-body co-registration of the neuromelanin-MRI image to the T1w; (7) application of the T1w MNI-transform to normalize the neuromelanin-MRI to MNI space and resampling to 1 mm isotropic resolution; (8) spatial smoothing with a 1 mm FWHM Gaussian kernel within the brain extraction mask using AFNI.

Finally, neuromelanin-MRI contrast ratio (CNR) maps were created to normalize signal intensity relative to the crus cerebri (CC); [21], a white matter region adjacent to the SN/VTA known to have negligible neuromelanin concentration. Specifically, CNR at each voxel was calculated as $(\text{signal} - \text{reference})/\text{reference} * 100$, such that the reference was the modal (based on a kernel distribution fit) signal intensity in a mask of the CC. CNR maps were visually checked for quality.

Analysis

Voxel-wise analyses examining CNR were performed in MATLAB; all other analyses were performed in R [65]. All regression analyses controlled for a priori demographic covariates: age, sex assigned at birth (female, male), race (binary variable for White or not), Hispanic ethnicity (yes/no), and site/scanner (CU, UM scanner 1, UM scanner 2).

Voxel-wise analysis. Neuromelanin-MRI was analyzed within an over-inclusive SN/VTA mask (1807 voxels) [21]. Voxel-wise CNR outliers beyond the 0.1 and 99.9 percentiles across all participants were censored. Voxel-wise analyses were performed using robust linear regression in MATLAB (with iteratively reweighted-least squares that is more robust to outliers than ordinary least-squares), permutation testing, and unbiased effect size estimation, as in prior work [21, 33, 63]. Voxel-wise analyses were examined as our primary approach; this validated method avoids circularity and accounts for the functional heterogeneity in SN/VTA, i.e., functionally relevant subdivisions of dopaminergic pathways may not respect anatomical subnuclei definitions. Similar to permutation-based multiple comparisons correction for fMRI, the variable of interest was shuffled (while keeping the covariates constant) and the regression analysis was rerun across 10,000 permutations. Null distributions were created for the number of voxels significant at $p < 0.05$ by chance (separate one-sided tests for positive and negative effects). Analysis-level permutation-based p -values were determined using these null distributions, i.e., testing whether the number of significant voxels was greater than expected by chance.

Voxel-wise group differences. The primary voxel-wise analyses examined group differences in neuromelanin-MRI CNR as a function of OCD diagnosis (yes/no). Voxel-wise analyses covaried for the demographic covariates. Group difference analyses based on OCD diagnosis were determined to be significant if the number of significant voxels was greater than expected by chance at permutation-based $p < 0.025$ for positive or negative effects.

For significant effects, a leave-one-out cross-validation analysis was used to estimate unbiased effect sizes. Specifically, the same voxel-wise robust regression model as above was run $N = 135$ times removing one participant in each iteration; average CNR was extracted for each participant within significant voxels (two-sided $p < 0.05$) from the model excluding that participant. These CNR averages were used for visualization and post-hoc testing. Spatial overlap with specific midbrain subnuclei (VTA vs. SNpc) was determined based on a high-resolution probabilistic atlas [66].

Test-retest. We assessed test-retest reliability among the children with OCD who successfully completed two MRI scans. Specifically, linear mixed-effect models were run with a random intercept for participant and the intra-class correlation coefficient (ICC) was extracted, specifically two-way mixed, single score ICC(3,1) [67], as in prior work [33].

Symptom associations. Next, post-hoc regressions probed associations with symptom severity—within the OCD group using CY-BOCS total scores and across the sample using the OCI-CV (total sum scores, excluding three hoarding items). These analyses were re-confirmed at the voxel-level in supplementary analyses. Within the OCD group, we also explored associations with symptom duration (current age – age when symptoms began causing distress). An exploratory regularized regression was used to test for associations with particular symptom clusters (presence/absence of current contamination, aggression, sexual, hoarding, ordering, magical thinking, somatic, or religious obsessions). Specifically, a LASSO (least absolute shrinkage and selection operator; *glmnet* package) [68] approach was used to keep/retain potentially colinear symptom endorsements. The model was set to retain demographic covariates (penalty factor = 0) and determined best-fit when regularizing regression coefficients for eight binary variables of obsession types. Data and analysis code are available upon request.

RESULTS

Sample characteristics

Table 1 displays demographic and clinical characteristics of the sample split by presence of an OCD diagnosis. Children with OCD were slightly older and more likely to be White than those without OCD. As expected, OCI-CV scores were higher among the OCD group but with varying non-zero scores among youth without

Table 1. Sample characteristics by group.

	No OCD ($N = 71$)	OCD ($N = 64$)	Group diff.	ES
Site (UM)	40 (56.34%)	33 (51.56%)	$\chi^2 = 0.15$	OR = 0.83
Age (years)*	10.44 (2.18)	11.31 (2.03)	$t = 2.39$	$d = 0.41$
Sex (female)	44 (61.97%)	41 (64.06%)	$\chi^2 = 0.01$	OR = 1.09
Race: White	46 (64.79%)	52 (81.25%)	$\chi^2 = 3.79$	OR = 2.34
Race: Black	9 (12.68%)	2 (3.12%)	2.93	OR = 0.22
Race: Asian	4 (5.63%)	4 (6.25%)	0.00	OR = 1.12
Race: Multiracial	9 (12.68%)	4 (6.25%)	0.94	OR = 0.46
Ethnicity (Hispanic)	12 (16.9%)	5 (7.81%)	$\chi^2 = 1.77$	OR = 0.42
Parental Education (college)	59 (83.1%)	60 (93.75%)	$\chi^2 = 2.71$	OR = 3.03
OCI-CV***	5.53 (5.08)	17.09 (6.88)	$t = 10.99$	$d = 1.91$
CY-BOCS (worst ever)	–	28.47 (4.66)	–	–
CY-BOCS (past week)	–	25.62 (5.31)	–	–
CY-BOCS (post-treatment)	–	16.37 (6.78)	–	–
CY-BOCS Improvement	–	8.10 (5.67)	–	–
AoO Symptom Distress (years)	–	8.56 (2.56)	–	–
Duration Symptom Distress (years)	–	2.83 (2.2)	–	–

Characteristics of the $N = 135$ included participants are summarized here. Group differences (and corresponding effect size [ES]) based on presence of an OCD diagnosis are indicated; t -statistic and Cohen's d for continuous outcomes, chi-square and odds ratio [OR] for binary outcomes. $N = 1$ participant was missing OCI-CV scores and $n = 1$ was missing age of onset (AoO) when symptoms became distressing. Parental education indicated whether at least one parent had completed college.

* $p < 0.05$; ** $p < 0.01$; *** $p < 0.001$.

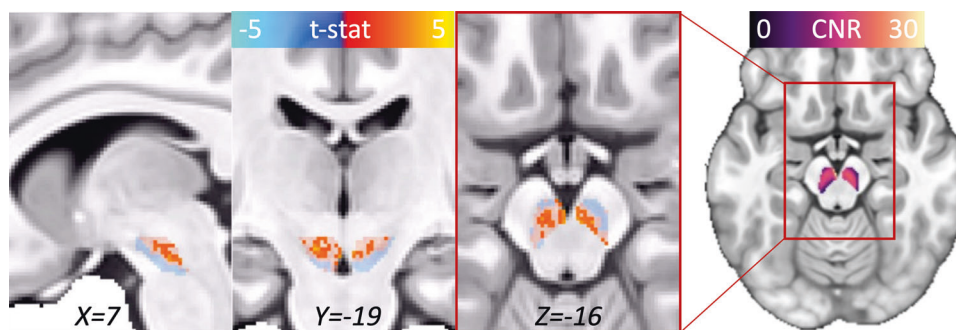


Fig. 1 Greater neuromelanin-MRI CNR among children with OCD. Voxel-wise group difference results are summarized here (centered at MNI 7, -19, -16). The t -statistic for the association with an OCD diagnosis (present > absent) is displayed voxel-wise within the SN/VTA analysis mask. Only the positive effect was significant at the analysis-level. Voxels significant at $p < 0.05$ are in opaque colors; non-significant voxels are more transparent. The left side images are a zoomed inset; average contrast-to-noise (0–30%) within the SN/VTA analysis mask is shown on the right-side axial view.

OCD. Seven of the children in the OCD group had a lifetime history of an ADHD diagnosis as well as of medication treatment for ADHD. Supplementary Table S1 displays differences by site; participants at the New York City site were more likely to identify as Hispanic.

Group differences in neuromelanin-MRI

Voxel-wise robust regression analyses indicated significantly higher neuromelanin-MRI CNR among children with OCD compared to those without (483 of 1807 SN/VTA voxels, permutation-corrected $p = 0.018$; Figs. 1 and 2a), controlling for demographic covariates. Post-hoc analysis of the average group difference effect from leave-one-out analyses is shown in Table 2 (Cohen's $d = 0.50$). Prior SSRI use and ADHD diagnosis/medication use did not relate to average CNR ($t < |0.55|$, $p > 0.59$) and adding medication use as an additional regression covariate did not affect the average group difference in CNR ($t = 2.74$, $p = 0.007$, Cohen's $d = 0.49$). These and additional sensitivity analyses indicating non-significant group \times age and group \times sex interactions are shown in Supplementary Table S2. Significant voxels covered much of the SNpc (33%) and the majority of the VTA (79%) atlas masks. Examining average CNR from significant voxels split within each atlas mask, group differences were observed in each subnuclei (SNpc: $t = 2.90$, $p = 0.004$, Cohen's $d = 0.51$; VTA: $t = 2.80$, $p = 0.006$, Cohen's $d = 0.50$).

Longitudinal effects

As expected, participants with OCD showed significant reduction in CY-BOCS from pre- to post-CBT ($t(58) = 10.97$, $p < .001$, Cohen's $d = 1.44$). CNR within the above significant cluster exhibited excellent reliability ($n = 47$ children with OCD; average voxel-wise ICC(3,1) = 0.85; Supplementary Fig. S2) over three months ($M = 15.6$ [SD = 2.88] weeks between scans). Change in neuromelanin CNR (residualized for baseline CNR) in this sample did not relate significantly to the number of days between scans ($t = 0.59$, $p = 0.55$) nor to improvement in CY-BOCS with treatment ($t = 1.01$, $p = 0.31$).

Symptom association

Average CNR from the cluster exhibiting significant group differences (extracted based on unbiased leave-one-out analyses) associated inversely with lifetime CY-BOCS symptom severity in the OCD group ($t = -2.72$, $p = 0.009$; $n = 64$; Fig. 2b), controlling for demographic covariates. Supplementary voxel-wise results confirmed this inverse association in an overlapping cluster (Supplementary Fig. S3). Average CNR was unassociated with past-week CY-BOCS severity ($t = -1.22$, $p = 0.23$; $n = 63$) or improvement in CY-BOCS with CBT ($t = 0.37$, $p = 0.71$, $n = 59$).

Longer illness duration (years since symptoms became distressing) also related to lower average CNR within the OCD group ($t = -2.22$, $p = 0.03$; $n = 63$; Fig. 2c). CY-BOCS and symptom duration were uncorrelated ($r = -0.01$, $t(61) = -0.04$, $p = 0.97$) and both significantly accounted for separable variance in average neuromelanin-MRI CNR when entered in the same model (Table 2). An exploratory LASSO regression within the OCD group retained four obsession domains of potential interest. The final model (Supplementary Table S3) highlighted associations between lower average neuromelanin-MRI CNR and the endorsement of ordering, sexual, and somatic obsessions; whereas, hoarding obsessions were associated with higher average neuromelanin-MRI CNR. Note that there were no significant differences in demographics or clinical severity among children with or without hoarding obsessions (Supplementary Table S4).

To examine potential associations with (sub)clinical symptom levels across the whole sample, OCI-CV scores were examined in relation to neuromelanin-MRI. CY-BOCS and OCI-CV scores were correlated in the OCD group ($r = 0.25$, $t(62) = 2.07$, $p = 0.04$). In a regression controlling for demographic covariates, an interaction between OCD diagnosis (absent/present) and OCI-CV total scores ($t = -2.25$, $p = 0.03$; $n = 134$; Fig. 2d) emerged, such that subclinical symptom levels associated positively with average CNR among children without OCD but negatively among those with an OCD diagnosis. This also may reflect an inverted-U-shaped association between symptoms and average CNR across the full sample (quadratic OCI term: $t = -2.08$, $p = 0.04$). Supplementary voxel-wise results confirmed this quadratic effect in an overlapping cluster (Supplementary Fig. S4).

DISCUSSION

This study represents the first indication of the utility of neuromelanin-MRI in pediatric psychiatry, specifically highlighting midbrain dopaminergic alterations in treatment-seeking youth with OCD. Adding to a burgeoning body of work examining neuromelanin-MRI as an in vivo marker of midbrain dopamine in adult samples, these results contribute novel insight into the neurobiology of OCD and pave the way toward future investigations of pediatric mental health. Particularly, we highlight greater neuromelanin-MRI signal in the midbrain in treatment-seeking youth with a diagnosis of OCD compared to youth without OCD, leveraging a relatively large sample of 6–14-year-old children across two sites to increase generalizability.

Dopamine is a critical neurotransmitter with widespread impact on neurocognitive function. Pharmacological and other manipulations of dopamine have been linked to many outcomes, including increases in repetitive behaviors [15–17, 19]. Accordingly, a small

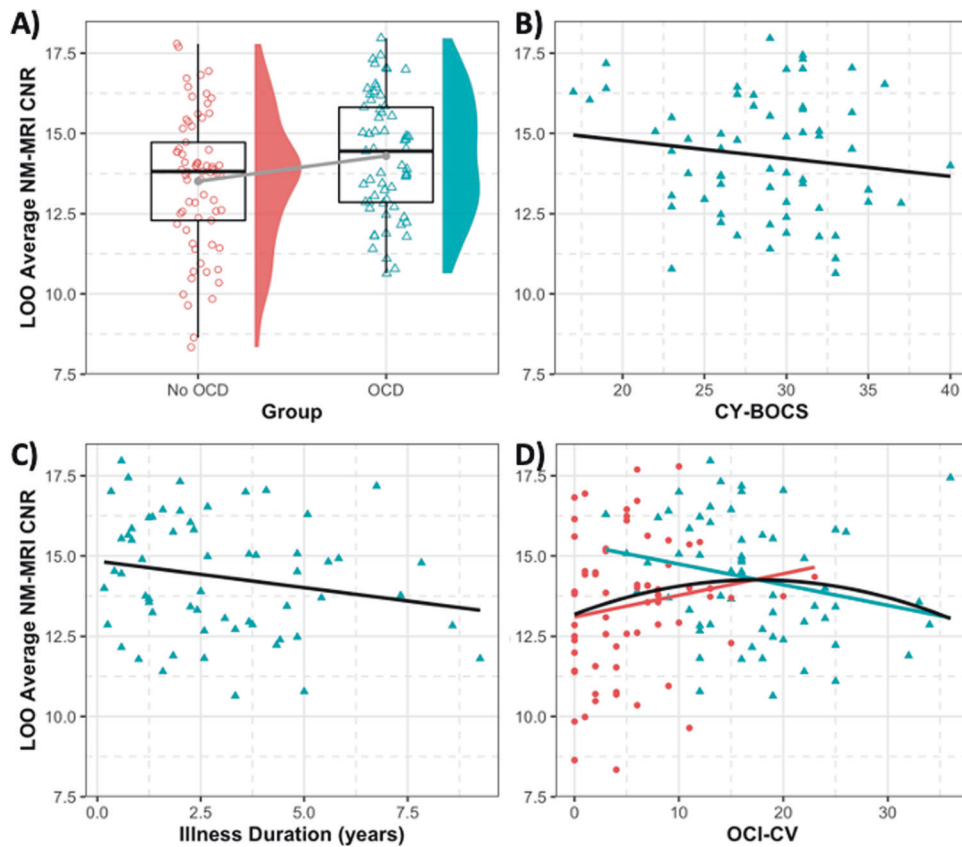


Fig. 2 Group differences and symptom associations with neuromelanin-MRI CNR. Average neuromelanin-MRI CNR was estimated from the leave-one-out (LOO) analyses and used for post-hoc testing. Group differences based on OCD diagnosis are displayed in panel **A**. Panel **B** displays associations between neuromelanin-MRI CNR and worst-ever symptom severity within the OCD group based on the Children's Yale-Brown Obsessive-Compulsive Scale (CY-BOCS). Panel **C** displays associations with illness duration (years since age when symptoms became distressing) among the OCD group. Associations with Obsessive-Compulsive Inventory-Children's Version (OCI-CV) scores are presented in panel **D** with linear fits within group and a quadratic fit across the sample. Youth with OCD are displayed with blue triangle markers and those without are displayed by red circles.

but growing body of work has suggested dopaminergic alterations in adult OCD [5–8], particularly increased striatal dopamine [9–14]. Dopaminergic alterations likely contribute to fronto-striatal circuit alterations often seen in OCD [8]. Yet, prior findings are at times mixed or rely on small samples of adult patients. In line with these prior findings, we also detected greater neuromelanin-MRI contrast—a proxy for midbrain dopamine—in youth with OCD. These findings persisted after controlling for demographic covariates and site differences. Significantly greater neuromelanin-MRI signal was observed for youth with OCD across a majority of the midbrain, implicating both the SNpc and VTA bilaterally. Dopamine neurons of the SNpc and VTA project to the striatum, perhaps contributing to the elevated endogenous striatal dopamine levels implicated in prior adult work [10, 13].

Among youth with OCD, average neuromelanin-MRI signal associated inversely with both lifetime symptom severity and illness duration. These findings were observed both in the cluster exhibiting group differences and in an overlapping cluster revealed from supplementary voxel-wise analyses. In conjunction with the main group differences, several interpretations are possible that can be probed in future work. First, though greater dopaminergic function was implicated in youth with OCD, increasingly high levels may incur compensatory benefits, i.e., youth with OCD and the highest neuromelanin-MRI signal exhibited the lowest symptom severity. This may also contribute to the negative association with illness duration, i.e., those with the longest duration may have the least compensatory benefit of greater dopaminergic function. Alternatively, effects might change

over the course of illness, such that dopaminergic function is highest closer to onset and decreases are noted with longer, recurrent course. Future work may aim to parse differentiable hypotheses favoring either (a) different associations or mechanisms present in youth with vs. without OCD (i.e., a group interaction) or (b) changes over the course of illness.

Another interpretation is that these results reflect heterogeneity among youth with OCD. In exploratory analyses, we found that endorsement of most types of obsessions associated with lower neuromelanin-MRI signal, as did overall severity scores. Note that certain types of obsessions were frequently endorsed (e.g., aggression and contamination), potentially limiting our ability to isolate separable or specific effects (Table S3). Nonetheless, current hoarding obsessions did appear to exhibit a separable effect, relating to higher neuromelanin-MRI signal among youth with OCD. Though research is limited, there is evidence linking dopaminergic function with hoarding [69–73]. Furthermore, the status of hoarding within OCD or as a separable disorder has been much debated [74–78]. Particularly, hoarding may be a particularly egosyntonic symptom within OCD, i.e., an intrinsically more rewarding obsession that is compatible with one's self identity and way of thinking, compared to other more distressing and unacceptable obsessions that are inconsistent with one's self-concept [79–85].

Neuromelanin-MRI likely reflects long-term alterations in dopaminergic function as neuromelanin accumulates across the lifespan [55, 86, 87]. In line with this, we observed high test-retest reliability in signal over several months and associations with

Table 2. Regression results predicting to neuromelanin-MRI CNR.

	Model 1: Group difference			Model 2: Severity within OCD group		
	Beta	T-stat	p	Beta	T-stat	p
Age	−0.14	−1.60	0.111	0.13	1.03	0.307
Sex (female)	0.31	1.75	0.082	0.10	0.39	0.699
Race (White)	−0.03	−0.18	0.860	−0.34	−1.24	0.222
Ethnicity (Hispanic)	0.05	0.17	0.863	0.11	0.26	0.793
Scanner - UM1	0.45	1.64	0.103	1.04	4.34	<0.001
Scanner - UM2	0.51	2.79	0.006	1.23	3.40	0.001
OCD	0.48	2.79	0.006	–	–	–
CY-BOCS	–	–	–	−0.29	−2.48	0.016
Symptom Duration (years)	–	–	–	−0.26	−2.27	0.027
R ² /R ² adjusted	0.15/0.10	N = 135		0.40/0.31	N = 64	
Model F	3.29	df = 127		4.48	df = 54	
Model p	0.003			<0.001		

Post-hoc linear regression results are displayed examining average neuromelanin-MRI CNR from the leave-one-out analyses following up on the main voxel-wise analysis (Fig. 1). The standardized regression coefficient (Beta) is displayed for each predictor with its corresponding *t*-statistic and *p*-value. Model 1 confirms the significant voxel-wise group difference, indicating greater CNR based on an OCD diagnosis (present > absent). Model 2 probes associations with lifetime symptom severity (CY-BOCS) and symptom duration (years) within the OCD group. *p*-values for effects of interest are emphasized in bold.

lifetime symptom severity and illness duration among youth with OCD. Particularly, neuromelanin-MRI signal was more strongly associated with lifetime peak severity rather than with current symptoms at baseline. Furthermore, despite the significant reduction in symptoms following CBT, neuromelanin-MRI signal was not associated with treatment response. Compared to more state-dependent indices like PET or task-based fMRI that can show acute fluctuations with current symptoms, neuromelanin-MRI may better index trait-like phenotypes [88] that make it well-suited as a stable early biomarker or predictor of long-term risk.

Several limitations may be noted for the current study. First, though our neuromelanin-MRI protocol has been well validated as a non-invasive proxy measure for midbrain neuromelanin and associated dopamine function [21, 22], we acknowledge this type of MRI approach cannot be fully specific to neuromelanin content and other anatomical or physiological factors may impact neuromelanin-MRI signal, e.g., free water content and cell morphology [89, 90]. Further studies are needed to examine different contributions of such processes to neuromelanin-MRI and if these play a role in OCD pathophysiology. Next, although a relatively large sample of treatment-seeking youth with OCD was assessed across two sites, future studies should aim to replicate these results in larger samples. Due to the COVID-19 pandemic, our sample size was also restricted for second MRI scans; future work can examine changes over time in a larger subset and over longer timespans. Last, the current study included a group of children with only a primary diagnosis of OCD; future work can include more heterogeneous samples to parse potential specificity of midbrain dopaminergic alterations to OCD relative to other frequently comorbid disorders, including anxiety and ADHD.

Overall, the role of dopamine has been understudied in OCD, especially pediatric OCD. We leveraged neuromelanin-MRI as a novel and reliable means of non-invasive assessment optimal for pediatric research. Though we do not observe strong associations with CBT response as we have seen with other neuroimaging modalities [91–95], future work may aim to probe neuromelanin-MRI as a predictor of efficacy of dopamine-based pharmacotherapy for example [96] or to otherwise help personalize care for particular subsets of patients (e.g., with or without hoarding). Furthermore, work can continue to investigate how early in development neuromelanin-MRI may begin to indicate OCD or

associated risk before illness onset as well as potential causes and consequences of dopaminergic alterations in youth with OCD.

REFERENCES

- Abudy A, Juven-Wetzler A, Sonnino R, Zohar J. Serotonin and beyond: a neurotransmitter perspective of OCD. In: *Obsessive-compulsive disorder*. Chichester, UK: John Wiley & Sons, Ltd; 2012. 220–43.
- Sinopoli VM, Burton CL, Kronenberg S, Arnold PD. A review of the role of serotonin system genes in obsessive-compulsive disorder. *Neurosci Biobehav Rev*. 2017;80:372–81.
- Ivarsson T, Skarphedinsson G, Kornør H, Axelsdottir B, Biedilæ S, Heyman I, et al. The place of and evidence for serotonin reuptake inhibitors (SRIs) for obsessive compulsive disorder (OCD) in children and adolescents: Views based on a systematic review and meta-analysis. *Psychiatry Res*. 2015;227:93–103.
- Kotapati VP, Khan AM, Dar S, Begum G, Bachu R, Adnan M, et al. The effectiveness of selective serotonin reuptake inhibitors for treatment of obsessive-compulsive disorder in adolescents and children: a systematic review and meta-analysis. *Front Psychiatry*. 2019;10:523.
- Koo MS, Kim EJ, Roh D, Kim CH. Role of dopamine in the pathophysiology and treatment of obsessive-compulsive disorder. *Expert Rev Neurother*. 2010;10:275–90.
- Denys D, Zohar J, Westenberg HG. The role of dopamine in obsessive-compulsive disorder: preclinical and clinical evidence. *J Clin Psychiatry*. 2004;65:11–7.
- Westenberg HGM, Fineberg NA, Denys D. Neurobiology of obsessive-compulsive disorder: *serotonin and beyond*. *CNS Spectr*. 2007;12:14–27.
- Wood J, Ahmari SE. A framework for understanding the emerging role of corticolimbic-ventral striatal networks in OCD-associated repetitive behaviors. *Front Syst Neurosci*. 2015;9:171.
- Hesse S, Muller U, Lincke T, Barthel H, Villmann T, Angermeyer MC, et al. Serotonin and dopamine transporter imaging in patients with obsessive-compulsive disorder. *Psychiatry Res*. 2005;140:63–72.
- Perani D, Garibotto V, Gorini A, Moresco RM, Henin M, Panzacchi A, et al. In vivo PET study of 5HT(2A) serotonin and D(2) dopamine dysfunction in drug-naïve obsessive-compulsive disorder. *Neuroimage*. 2008;42:306–14.
- Olver JS, O'Keefe G, Jones GR, Burrows GD, Tochon-Danguy HJ, Ackermann U, et al. Dopamine D1 receptor binding in the striatum of patients with obsessive-compulsive disorder. *J Affect Disord*. 2009;114:321–6.
- Kim C-H, Koo M-S, Cheon K-A, Ryu Y-H, Lee J-D, Lee H-S. Dopamine transporter density of basal ganglia assessed with [123I]IPT SPET in obsessive-compulsive disorder. *Eur J Nucl Med Mol Imaging*. 2003;30:1637–43.
- Denys D, de Vries F, Cath D, Figeo M, Vulink N, Veltman DJ, et al. Dopaminergic activity in Tourette syndrome and obsessive-compulsive disorder. *Eur Neuropsychopharmacol*. 2013;23:1423–31.
- van der Wee NJ, Stevens H, Hardeman JA, Mandl RC, Denys DA, van Megen HJ, et al. Enhanced dopamine transporter density in psychotropic-naïve patients

- with obsessive-compulsive disorder shown by [123I]beta-CIT SPECT. *Am J Psychiatry*. 2004;161:2201–6.
15. Voon V, Potenza MN, Thomsen T. Medication-related impulse control and repetitive behaviors in Parkinson's disease. *Curr Opin Neurol*. 2007;20:484–92.
 16. Voon V, Fox SH. Medication-related impulse control and repetitive behaviors in Parkinson disease. *Arch Neurol*. 2007;64:1089–96.
 17. Sesia T, Bizup B, Grace AA. Evaluation of animal models of obsessive-compulsive disorder: correlation with phasic dopamine neuron activity. *Int J Neuropsychopharmacol*. 2013;16:1295–307.
 18. Turk AZ, Lotfi Marchoubeh M, Fritsch I, Maguire GA, SheikhBahaei S. Dopamine, vocalization, and astrocytes. *Brain Lang*. 2021;219:104970.
 19. Kaluuff AV, Stewart AM, Song C, Berridge KC, Graybiel AM, Fentress JC. Neurobiology of rodent self-grooming and its value for translational neuroscience. *Nat Rev Neurosci*. 2016;17:45–59.
 20. Cools R, D'Esposito M. Inverted-U-shaped dopamine actions on human working memory and cognitive control. *Biol Psychiatry*. 2011;69:e113–e125.
 21. Cassidy CM, Zucca FA, Girgis RR, Baker SC, Weinstein JJ, Sharp ME, et al. Neuromelanin-sensitive MRI as a noninvasive proxy measure of dopamine function in the human brain. *Proc Natl Acad Sci USA*. 2019;116:5108–17.
 22. Sulzer D, Cassidy C, Horga G, Kang UJ, Fahn S, Casella L, et al. Neuromelanin detection by magnetic resonance imaging (MRI) and its promise as a biomarker for Parkinson's disease. *NPJ Parkinsons Dis*. 2018;4:11.
 23. Poulin J-F, Caronia G, Hofer C, Cui Q, Helm B, Ramakrishnan C, et al. Mapping projections of molecularly defined dopamine neuron subtypes using intersectional genetic approaches. *Nat Neurosci*. 2018;21:1260–71.
 24. Sonne J, Reddy V, Beato MR. *Neuroanatomy, Substantia Nigra*. StatPearls: StatPearls Publishing; 2021.
 25. Moore RY, Bloom FE. Central catecholamine neuron systems: anatomy and physiology of the dopamine systems. *Annu Rev Neurosci*. 1978;1:129–69.
 26. Meiser J, Weindl D, Hiller K. Complexity of dopamine metabolism. *Cell Commun Signal*. 2013;11:34.
 27. Zecca L, Zucca FA, Wilms H, Sulzer D. Neuromelanin of the substantia nigra: a neuronal black hole with protective and toxic characteristics. *Trends Neurosci*. 2003;26:578–80.
 28. Zecca L, Tampellini D, Gerlach M, Riederer P, Fariello RG, Sulzer D. Substantia nigra neuromelanin: structure, synthesis, and molecular behaviour. *Mol Pathol*. 2001;54:414–8.
 29. Sulzer D, Bogulavsky J, Larsen KE, Behr G, Karatekin E, Kleinman MH, et al. Neuromelanin biosynthesis is driven by excess cytosolic catecholamines not accumulated by synaptic vesicles. *Proc Natl Acad Sci USA*. 2000;97:11869–74.
 30. Brammerloh M, Morawski M, Weigelt I, Reinert T, Lange C, Pelicon P, et al. Toward an early diagnostic marker of Parkinson's: measuring iron in dopaminergic neurons with MR relaxometry. *bioRxiv*. 2020. <https://doi.org/10.1101/2020.07.01.170563>.
 31. Ito H, Kawaguchi H, Kodaka F, Takuwa H, Ikoma Y, Shimada H, et al. Normative data of dopaminergic neurotransmission functions in substantia nigra measured with MRI and PET: Neuromelanin, dopamine synthesis, dopamine transporters, and dopamine D2 receptors. *Neuroimage*. 2017;158:12–7.
 32. Langley J, Huddleston DE, Chen X, Sedlacki J, Zachariah N, Hu X. A multicontrast approach for comprehensive imaging of substantia nigra. *Neuroimage*. 2015;112:7–13.
 33. Wengler K, He X, Abi-Dargham A, Horga G. Reproducibility assessment of neuromelanin-sensitive magnetic resonance imaging protocols for region-of-interest and voxelwise analyses. *Neuroimage*. 2019;208:116457.
 34. van der Pluijm M, Cassidy C, Zandstra M, Wallert E, de Bruin K, Booij J, et al. Reliability and reproducibility of neuromelanin-sensitive imaging of the substantia nigra: a comparison of three different sequences. *J Magn Reson Imaging*. 2021;53:712–21.
 35. Castellanos G, Fernandez-Seara MA, Lorenzo-Betancor O, Ortega-Cubero S, Puigvert M, Uranga J, et al. Automated neuromelanin imaging as a diagnostic biomarker for Parkinson's disease. *Mov Disord*. 2015;30:945–52.
 36. Kawaguchi H, Shimada H, Kodaka F, Suzuki M, Shinotoh H, Hirano S, et al. Principal component analysis of multimodal neuromelanin MRI and dopamine transporter PET data provides a specific metric for the nigral dopaminergic neuronal density. *PLoS One*. 2016;11:e0151191.
 37. Sasaki M, Shibata E, Tohyama K, Takahashi J, Otsuka K, Tsuchiya K, et al. Neuromelanin magnetic resonance imaging of locus coeruleus and substantia nigra in Parkinson's disease. *Neuroreport*. 2006;17:1215–8.
 38. Cho SJ, Bae YJ, Kim JM, Kim D, Baik SH, Sunwoo L, et al. Diagnostic performance of neuromelanin-sensitive magnetic resonance imaging for patients with Parkinson's disease and factor analysis for its heterogeneity: a systematic review and meta-analysis. *Eur Radio*. 2021;31:1268–80.
 39. Wang L, Yan Y, Zhang L, Liu Y, Luo R, Chang Y. Substantia nigra neuromelanin magnetic resonance imaging in patients with different subtypes of Parkinson disease. *J Neural Transm*. 2021. <https://doi.org/10.1007/s00702-020-02295-8>.
 40. Biondetti E, Gaurav R, Yahia-Cherif L, Mangone G, Pyatigorskaya N, Valabregue R, et al. Spatiotemporal changes in substantia nigra neuromelanin content in Parkinson's disease. *Brain*. 2020;143:2757–70.
 41. Kashihara K, Shinya T, Higaki F. Neuromelanin magnetic resonance imaging of nigral volume loss in patients with Parkinson's disease. *J Clin Neurosci*. 2011;18:1093–6.
 42. Ohtsuka C, Sasaki M, Konno K, Kato K, Takahashi J, Yamashita F, et al. Differentiation of early-stage parkinsonisms using neuromelanin-sensitive magnetic resonance imaging. *Parkinsonism Relat Disord*. 2014;20:755–60.
 43. Ohtsuka C, Sasaki M, Konno K, Koide M, Kato K, Takahashi J, et al. Changes in substantia nigra and locus coeruleus in patients with early-stage Parkinson's disease using neuromelanin-sensitive MR imaging. *Neurosci Lett*. 2013;541:93–8.
 44. Reimão S, Ferreira S, Nunes RG, Pita Lobo P, Neutel D, Abreu D, et al. Magnetic resonance correlation of iron content with neuromelanin in the substantia nigra of early-stage Parkinson's disease. *Eur J Neurol*. 2016;23:368–74.
 45. Safai A, Prasad S, Chougule T, Saini J, Pal PK, Ingalhalikar M. Microstructural abnormalities of substantia nigra in Parkinson's disease: A neuromelanin sensitive MRI atlas based study. *Hum Brain Mapp*. 2020;41:1323–33.
 46. Hirsch E, Graybiel AM, Agid YA. Melanized dopaminergic neurons are differentially susceptible to degeneration in Parkinson's disease. *Nature*. 1988;334:345–8.
 47. Shibata E, Sasaki M, Tohyama K, Otsuka K, Endoh J, Terayama Y, et al. Use of neuromelanin-sensitive MRI to distinguish schizophrenic and depressive patients and healthy individuals based on signal alterations in the substantia nigra and locus coeruleus. *Biol Psychiatry*. 2008;64:401–6.
 48. Watanabe Y, Tanaka H, Tsukabe A, Kunitomi Y, Nishizawa M, Hashimoto R, et al. Neuromelanin magnetic resonance imaging reveals increased dopaminergic neuron activity in the substantia nigra of patients with schizophrenia. *PLoS One*. 2014;9:e104619.
 49. Yamashita F, Sasaki M, Fukumoto K, Otsuka K, Uwano I, Kameda H, et al. Detection of changes in the ventral tegmental area of patients with schizophrenia using neuromelanin-sensitive MRI. *Neuroreport*. 2016;27:289–94.
 50. Jalles C, Chendo I, Levy P, Reimão S. Neuromelanin changes in first episode psychosis with substance abuse. *Schizophr Res*. 2020;220:283–4.
 51. Ueno F, Iwata Y, Nakajima S, Caravaggio F, Rubio JM, Horga G, et al. Neuromelanin accumulation in patients with schizophrenia: A systematic review and meta-analysis. *Neurosci Biobehav Rev*. 2022;132:1205–13.
 52. Van Der Pluijm M, De Haan L, Booij J, Van de Giessen E. Neuromelanin MRI as biomarker for treatment resistance in first episode schizophrenia patients. *Neurosci Appl*. 2022;1:100077.
 53. Tavares M, Reimão S, Chendo I, Carvalho M, Levy P, Nunes RG. Neuromelanin magnetic resonance imaging of the substantia nigra in first episode psychosis patients consumers of illicit substances. *Schizophr Res*. 2018;197:620–1.
 54. Meltzer HY, Stahl SM. The dopamine hypothesis of schizophrenia: a review. *Schizophr Bull*. 1976;2:19–76.
 55. Zecca L, Fariello R, Riederer P, Sulzer D, Gatti A, Tampellini D. The absolute concentration of nigral neuromelanin, assayed by a new sensitive method, increases throughout the life and is dramatically decreased in Parkinson's disease. *FEBS Lett*. 2002;510:216–20.
 56. March JS, Franklin M, Nelson A, Foa E. Cognitive-behavioral psychotherapy for pediatric obsessive-compulsive disorder. *J Clin Child Psychol*. 2001;30:8–18.
 57. March JS, Mulle K. OCD in children and adolescents. New York, NY: Guilford Publications; 1998.
 58. Kaufman J, Birmaher B, Brent D, Rao UMA, Flynn C, Moreci P, et al. Schedule for affective disorders and schizophrenia for school-age children-present and lifetime version (K-SADS-PL): initial reliability and validity data. *J Am Acad Child Adolesc Psychiatry*. 1997;36:980–8.
 59. Scahill L, Riddle MA, McSwiggin-Hardin M, Ort SI, King RA, Goodman WK, et al. Children's Yale-Brown Obsessive Compulsive Scale: reliability and validity. *J Am Acad Child Adolesc Psychiatry*. 1997;36:844–52.
 60. Hanna GL. Schedule for obsessive-compulsive and other behavioral syndromes (SOCOBS). Ann Arbor, MI: University of Michigan; 2013.
 61. Foa EB, Coles M, Huppert JD, Pasupuleti RV, Franklin ME, March J. Development and validation of a child version of the obsessive compulsive inventory. *Behav Ther*. 2010;41:121–32.
 62. Casey BJ, Cannonier T, Conley MI, Cohen AO, Barch DM, Heitzeg MM, et al. The Adolescent Brain Cognitive Development (ABCD) study: Imaging acquisition across 21 sites. *Dev Cogn Neurosci*. 2018;32:43–54.
 63. Wengler K, Ashinoff BK, Pueraro E, Cassidy CM, Horga G, Rutherford BR. Association between neuromelanin-sensitive MRI signal and psychomotor slowing in late-life depression. *Neuropsychopharmacology*. 2021;46:1233–9.
 64. Salzman G, Kim J, Horga G, Wengler K. Standardized data acquisition for neuromelanin-sensitive magnetic resonance imaging of the substantia nigra. *J Vis Exp*. 2021. <https://doi.org/10.3791/62493>.
 65. R Core Team. R: A language and environment for statistical computing. Vienna: R Foundation for Statistical Computing; 2020. <https://www.R-project.org/>.

66. Pauli WM, Nili AN, Tyszka JM. A high-resolution probabilistic in vivo atlas of human subcortical brain nuclei. *Sci Data*. 2018;5:180063.
67. Shrout PE, Fleiss JL. Intraclass correlations: uses in assessing rater reliability. *Psychol Bull*. 1979;86:420–8.
68. Friedman J, Hastie T, Tibshirani R. Regularization paths for generalized linear models via coordinate descent. *J Stat Softw*. 2010;33:1–22.
69. Kelley AE, Stinus L. Disappearance of hoarding behavior after 6-hydroxydopamine lesions of the mesolimbic dopamine neurons and its reinstatement with l-dopa. *Behav Neurosci*. 1985;99:531–45.
70. McLaughlin T, Blum K, Steinberg B, Modestino EJ, Fried L, Baron D, et al. Pro-dopamine regulator, KB220Z, attenuates hoarding and shopping behavior in a female, diagnosed with SUD and ADHD. *J Behav Addict*. 2018;7:192–203.
71. O'Sullivan SS, Djamshidian A, Evans AH, Loane CM, Lees AJ, Lawrence AD. Excessive hoarding in Parkinson's disease. *Mov Disord*. 2010;25:1026–33.
72. Yang H-D, Wang Q, Wang Z, Wang D-H. Food hoarding and associated neuronal activation in brain reward circuitry in Mongolian gerbils. *Physiol Behav*. 2011;104:429–36.
73. Stein DJ, Seedat S, Potocnik F. Hoarding: a review. *Isr J Psychiatry Relat Sci*. 1999;36:35–46.
74. Abramowitz JS, Wheaton MG, Storch EA. The status of hoarding as a symptom of obsessive-compulsive disorder. *Behav Res Ther*. 2008;46:1026–33.
75. Pertusa A, Fullana MA, Singh S, Alonso P, Menchón JM, Mataix-Cols D. Compulsive hoarding: OCD symptom, distinct clinical syndrome, or both? *Am J Psychiatry*. 2008;165:1289–98.
76. Rachman S, Elliott CM, Shafran R, Radomsky AS. Separating hoarding from OCD. *Behav Res Ther*. 2009;47:520–2.
77. Samuels JF, Bienvenu OJ III, Pinto A, Fyer AJ, McCracken JT, Rauch SL, et al. Hoarding in obsessive-compulsive disorder: results from the OCD Collaborative Genetics Study. *Behav Res Ther*. 2007;45:673–86.
78. Mataix-Cols D, Frost RO, Pertusa A, Clark LA, Saxena S, Leckman JF, et al. Hoarding disorder: a new diagnosis for DSM-V? *Depress Anxiety*. 2010;27:556–72.
79. Kellett S, Greenhalgh R, Beail N, Ridgway N. Compulsive hoarding: an interpretative phenomenological analysis. *Behav Cogn Psychother*. 2010;38:141–55.
80. Black DW, Monahan P, Gable J, Blum N, Clancy G, Baker P. Hoarding and treatment response in 38 nondepressed subjects with obsessive-compulsive disorder. *J Clin Psychiatry*. 1998;59:420–5.
81. Kings CA, Moulding R, Knight T. You are what you own: reviewing the link between possessions, emotional attachment, and the self-concept in hoarding disorder. *J Obsessive Compuls Relat Disord*. 2017;14:51–8.
82. Seedat S, Stein DJ. Hoarding in obsessive-compulsive disorder and related disorders: a preliminary report of 15 cases. *Psychiatry Clin Neurosci*. 2002;56:17–23.
83. Frost RO, Gross RC. The hoarding of possessions. *Behav Res Ther*. 1993;31:367–81.
84. Grisham JR, Brown TA, Liverant GI, Campbell-Sills L. The distinctiveness of compulsive hoarding from obsessive-compulsive disorder. *J Anxiety Disord*. 2005;19:767–79.
85. Tolin DF. Understanding and treating hoarding: a biopsychosocial perspective. *J Clin Psychol*. 2011;67:517–26.
86. Shibata E, Sasaki M, Tohyama K, Kanbara Y, Otsuka K, Ehara S, et al. Age-related changes in locus ceruleus on neuromelanin magnetic resonance imaging at 3 Tesla. *Magn Reson Med Sci*. 2006;5:197–200.
87. Halliday GM, Fedorow H, Rickert CH, Gerlach M, Riederer P, Double KL. Evidence for specific phases in the development of human neuromelanin. *J Neural Transm*. 2006;113:721–8.
88. Horga G, Wengler K, Cassidy CM. Neuromelanin-sensitive magnetic resonance imaging as a proxy marker for catecholamine function in psychiatry. *JAMA Psychiatry*. 2021;78:788–9.
89. Trujillo P, Petersen KJ, Cronin MJ, Lin Y-C, Kang H, Donahue MJ, et al. Quantitative magnetization transfer imaging of the human locus coeruleus. *Neuroimage*. 2019;200:191–8.
90. Watanabe T, Tan Z, Wang X, Martinez-Hernandez A, Frahm J. Magnetic resonance imaging of noradrenergic neurons. *Brain Struct Funct*. 2019;224:1609–25.
91. Cyr M, Pagliaccio D, Yanes-Lukin P, Fontaine M, Rynn MA, Marsh R. Altered network connectivity predicts response to cognitive-behavioral therapy in pediatric obsessive-compulsive disorder. *Neuropsychopharmacology*. 2020;45:1232–40.
92. Cyr M, Pagliaccio D, Yanes-Lukin P, Goldberg P, Fontaine M, Rynn MA, et al. Altered fronto-amygdalar functional connectivity predicts response to cognitive behavioral therapy in pediatric obsessive-compulsive disorder. *Depress Anxiety*. 2021;38:836–45.
93. Pagliaccio D, Middleton R, Hezel D, Steinman S, Snorrason I, Gershkovich M, et al. Task-based fMRI predicts response and remission to exposure therapy in obsessive-compulsive disorder. *Proc Natl Acad Sci USA*. 2019;116:20346–53.
94. Pagliaccio D, Cha J, He X, Cyr M, Yanes-Lukin P, Goldberg P, et al. Structural neural markers of response to cognitive behavioral therapy in pediatric obsessive-compulsive disorder. *J Child Psychol Psychiatry*. 2020;61:1299–308.
95. Shi TC, Pagliaccio D, Cyr M, Simpson HB, Marsh R. Network-based functional connectivity predicts response to exposure therapy in unmedicated adults with obsessive-compulsive disorder. *Neuropsychopharmacology*. 2021;46:1035–44.
96. Ducasse D, Boyer L, Michel P, Loundou A, Macgregor A, Micoulaud-Franchi JA, et al. D2 and D3 dopamine receptor affinity predicts effectiveness of antipsychotic drugs in obsessive-compulsive disorders: a meta-regression analysis. *Psychopharmacology*. 2014;231:3765–70.

ACKNOWLEDGEMENTS

This work was partially supported by funds from the National Institute of Mental Health (R01 MH115024, Pls: Marsh & Fitzgerald) as was the efforts of the authors: Dr. Pagliaccio (R21 MH125044, R01 MH126181), Dr. Horga (R01 MH117323, R01 MH114965), Dr. Wengler (F32 MH125540). Preliminary findings from this work were presented at the 2021 meeting of the Society for Biological Psychiatry (<https://doi.org/10.1016/j.biopsych.2021.02.212>). The content is solely the responsibility of the authors and does not necessarily represent the official views of the National Institutes of Health. Dr. Pagliaccio confirms that he had full access to all the data in the study and takes responsibility for the integrity of the data and the accuracy of the data analysis.

AUTHOR CONTRIBUTIONS

DP analyzed study data and prepared the manuscript. KW and GH developed the neuromelanin-MRI protocol and processing pipeline. MF oversaw MRI data collection and quality control. KD, HB, and EB conducted and oversaw clinical assessment procedures. MR, SP, and CR collected study data and performed data quality control. DP, KDF, and RM designed the study and oversaw study procedures. All authors contributed to manuscript review and editing.

COMPETING INTERESTS

KW and GH report having filed patents for analysis and use of neuromelanin imaging in central nervous system disorders, licensed to Terran Biosciences, but have received no royalties. All other authors reported no biomedical financial interests or potential conflicts of interest.

ADDITIONAL INFORMATION

Supplementary information The online version contains supplementary material available at <https://doi.org/10.1038/s41380-023-02105-z>.

Correspondence and requests for materials should be addressed to David Pagliaccio.

Reprints and permission information is available at <http://www.nature.com/reprints>

Publisher's note Springer Nature remains neutral with regard to jurisdictional claims in published maps and institutional affiliations.

Springer Nature or its licensor (e.g. a society or other partner) holds exclusive rights to this article under a publishing agreement with the author(s) or other rightsholder(s); author self-archiving of the accepted manuscript version of this article is solely governed by the terms of such publishing agreement and applicable law.